# Decoupled Unknown Input Observer for Takagi-Sugeno Systems: Hardware-in-the-Loop Validation to Synchronous Reluctance Motor

**Wail Hamdi[1], Ramzi Saadi[1,*], Mohamed Yacine Hammoudi[1], Madina Hamiane[2]**
*[1]Laboratory of Energy Systems Modeling (LMSE), Department of Electrical Engineering, Mohamed KHIDER University of Biskra, B.P. 145 R.P. 07000, Biskra, Algeria*
*[2]College of Engineering, Royal University for Women, Al Muaskar Hwy, Riffa, Bahrein*
*wail.hamdi@univ-biskra.dz; *r.saadi@univ-biskra.dz; my.hammoudi@univ-biskra.dz; mhamiane@ruw.edu.bh*

***Abstract*—This paper introduces a decoupled unknown input observer (DUIO) for Takagi-Sugeno (T-S) systems, designed specifically for the synchronous reluctance motor (SynRM). The proposed DUIO method demonstrates enhanced robustness and accuracy in state estimation by effectively decoupling the influence of unknown inputs from the estimation error dynamics. Furthermore, the DUIO exhibits superior performance compared to the proportional integral observer (PIO) and the proportional multi-integral observer (PMIO) presented in previous studies, without the need for prior knowledge of the unknown input form or assumptions regarding its boundedness. Stability conditions, achieved using the quadratic Lyapunov function, are expressed as linear matrix inequalities (LMIs), which ensure asymptotic convergence of the estimation error. The effectiveness of the DUIO method is further validated in various scenarios through hardware-in-the-loop (HIL) implementation. This innovative approach significantly enhances the accuracy and reliability of SynRM state estimations and unknown input detections.**

***Index Terms*—Decoupled unknown input observer; Hardware-in-the-loop validation; Synchronous reluctance motor; Takagi-Sugeno fuzzy system.**

## I. INTRODUCTION

Synchronous reluctance motors (SynRMs) have gradually emerged as potential alternatives to traditional types of machines due to their commendable performance characteristics and resourceful utilities [1]. SynRMs are distinguished by their straightforward design, high efficiency, and significant torque density, which all contribute to their extensive use in various areas such as electric vehicles [2], [3], pump applications [4], [5], and industrial applications [6]. With a notable lack of permanent magnets and rotor windings, these motors boast improved reliability and reduced maintenance requirements, demonstrating their integral role in sustainable and energy-efficient power systems.

However, with the wide use of these systems, their robustness against potential faults and errors became prominent. In this regard, observers have played a significant role in enhancing the reliability and safety of industrial systems. These mathematical constructs have allowed for the estimation of both system states and unknown inputs (UIs), which could be indicative of faults. The importance of observers lies in their ability to swiftly detect and diagnose faults, thus minimising system downtime and mitigating adverse consequences. Estimating these UIs is critical as it facilitates a better understanding and control of the behaviours of the system, therefore leading to improved efficiency and system longevity [7]–[9].

The historical development of observers has been a journey of continuous innovation that goes back to the groundbreaking work of Kalman and Luenberger in their research papers in [10] and [11]. These seminal works were designed for linear systems; however, real-world systems often exhibit nonlinear behaviours, which poses a substantial challenge to the linear assumption. To address this issue, extended observers, such as the extended Luenberger observer and the extended Kalman filter, have emerged. These were developed in the basis of the linearisation method around an operational point, allowing them to handle mild nonlinearities. This approach enables the principles of the Kalman filter and the Luenberger observer to be applied to a broader class of systems. Despite their widespread use, these methods can struggle with highly nonlinear dynamics or systems that are not well suited for linearisation. In response to these limitations, several alternative methods have been developed. This paper uses the capabilities of the Takagi-Sugeno (T-S) fuzzy model, a powerful tool in the analysis of nonlinear systems, to estimate the state and UI [12]. The T-S models provide a comprehensible, systematic, and efficient approach to representation, identification [13], and control of complex nonlinear systems [14]. This method, through its linguistic rule base and continuous interpolation, provides enhanced flexibility and precision and has become a popular choice in control system studies [15]. The application of T-S models for UI estimation is the cornerstone of this work, which

Manuscript received 24 January, 2024; accepted 28 April, 2024.

demonstrates the capabilities of observer design in SynRM.

There are two main categories of UI observers in the existing literature. The first category encompasses simultaneous state and UI observers, such as proportional integral observers (PIO) and proportional multi-integral observers (PMIO), which have found broad application in various domains. For example, Abdelmalek Azar, and Dib [16] proposed the application of PIO for fault-tolerant control in doubly fed induction generator-based wind turbines. Boukhlouf, Hammoudi, Saadi, and Benbouzid [17] used the PIO to estimate the states and the UI in SynRM. Despite its widespread use, PIO has a significant limitation: It considers the UI to be either constant or with slow variation, according to the assumption that the first derivative of the UI equals zero. Consequently, when the UI variation is rapid, PIO can only deliver moderate results. The PMIO, on the other hand, is suitable for the polynomial UI form by considering the $q^{th}$ derivative of the UI to be zero; this characteristic contributes to enhancing the estimation precision of the UIs. The PMIO observer has been used recently in [18] to enhance the UI estimation of the SynRM. Although PMIO covers a broader class of UIs compared to PIO, it faces challenges when the order of the polynomial UI exceeds the design limit of the observer or when the form of the UI is nonpolynomial. In this paper, the second category of UI observer, the decoupled unknown input observer (DUIO), is adopted. DUIO separates the UI from the state estimation error and estimates them independently. Unlike other observers, DUIO does not require prior determination of the UI order, hence allowing for the estimation of a larger class of unknown signals. The comparative studies presented by the authors in [19] demonstrated DUIO's superiority over PMIO. In [20], the authors introduced a DUIO for discrete-time uncertain systems. They applied this to a DC motor controlling an inverted pendulum using a nonquadratic Lyapunov function, which offers less conservatism compared to the quadratic function. Despite its advantages, the DUIO decoupling strategy for SynRM has not been examined, which has motivated the authors of this paper to investigate the improvement of state and UI estimates compared to both the PIO proposed in [17] and the PMIO.

To validate the proposed method, hardware-in-the-loop (HIL) testing is implemented. HIL is a robust validation and testing methodology that incorporates real-time simulation to combine physical hardware and virtual modelling, thus enabling comprehensive analysis and testing of control systems. This procedure provides unique advantages, such as reducing the development cycle and costs, allowing safer and more flexible testing environments, and facilitating earlier detection and resolution of potential problems [21]–[23]. The application of HIL validation in this paper reinforces the robustness and reliability of the proposed DUIO method in the SynRM framework and opens up new avenues for future research and development in this field.

The key contribution of this work consists in enhancing the estimation of UIs in SynRM through the following.

– Design of an enhanced robust observer for state and UI estimation in SynRMs, achieved by effectively segregating the influence of the UI from the dynamics of the estimation error.

– Provide a higher accuracy in estimating UIs for SynRM, outperforming both the proportional integral observer proposed in [17] and the proportional multi-integral observer applied in [18]. Notably, this observer does not require prior knowledge of the form of the UI, nor does it assume that the input is bounded compared with the previous mentioned observers.

– The hardware-in-the-loop implementation was conducted to evaluate the performance of the proposed observer, comparing it with the PIO and the PMIO.

This paper comprises eight sections, each with a specific focus. Section II introduces the mathematical model of SynRM. Section III gives the Takagi-Sugeno fuzzy representation of the system. The DUIO structure and related stability conditions are explained in Section IV, while the methodology for UI estimation is discussed in Section V. Section VI explores the application of the proposed observer on the SynRM, and a real-time comparative test of DUIO, PIO, and PMIO is provided in Section VII. The article concludes in Section VIII with suggestions for future improvements.

## II. MATHEMATICAL MODEL OF SYNCHRONOUS RELUCTANCE MOTOR

The mathematical model of the synchronous reluctance motor in the rotational $d-q$ reference is given by the following [24]:

$$\begin{cases} V_{sd} = R_s i_{sd} + L_d \dfrac{di_{sd}}{dt} - \omega L_q i_{sq}, \\ V_{sq} = R_s i_{sq} + L_q \dfrac{di_{sq}}{dt} + \omega L_d i_{sd}, \\ \dfrac{d\omega}{dt} = \dfrac{3}{2}\dfrac{p^2}{J_m}\left(L_d - L_q\right) i_{sd} i_{sq} - \dfrac{f}{J_m}\omega - \dfrac{p}{J_m} T_L(t), \end{cases} \tag{1}$$

where $V_{sd}$ and $V_{sq}$ represent the direct and quadrature stator voltages, respectively; while $i_{sd}$ and $i_{sq}$ correspond to the direct and quadrature stator currents. $\omega$ refers to the electrical angular speed, and $T_L$ denotes the load torque. The remaining parameters are defined in Section VI.

By defining $x(t) = [i_{sd} \quad i_{sq} \quad \omega]$, $u(t) = [u_{sd} \quad u_{sq}]$, and $d(t) = T_L(t)$, the state-space representation of the dynamical model of the SynRM is as follows:

$$\begin{cases} \dot{x}(t) = A(x)x(t) + Bu(t) + Ed(t), \\ y(t) = Cx(t) + Gd(t), \end{cases} \tag{2}$$

where $x(t) \in \mathbb{R}^n$: the state vector, $u(t) \in \mathbb{R}^{n_u}$: the known input vector, $d(t) \in \mathbb{R}^{n_d}$: the UI vector $y(t) \in \mathbb{R}^{n_y}$: the output vector, $A(x) = \begin{bmatrix} -\dfrac{R_s}{L_d} & \dfrac{L_q}{L_d}\omega & 0 \\ -\dfrac{L_d}{L_q}\omega & -\dfrac{R_s}{L_q} & 0 \\ \alpha i_{sq} & 0 & -\dfrac{f}{J_m} \end{bmatrix}$,

$$\alpha = \frac{3p^2}{2J_m}\left(L_d - L_q\right), \qquad C = \begin{bmatrix} 0 & 0 & 1 \end{bmatrix}, \qquad B = \begin{bmatrix} \frac{1}{L_d} & 0 \\ 0 & \frac{1}{L_q} \\ 0 & 0 \end{bmatrix},$$

$$E = \begin{bmatrix} 0 \\ 0 \\ -\frac{p}{J_m} \end{bmatrix}, \text{ and } G = 0.$$

## III. TAKAGI-SUGENO FUZZY MODEL FOR THE SYNCHRONOUS RELUCTANCE MOTOR

The Takagi-Sugeno (T-S) model provides an effective capture of the complex nonlinear behaviours of SynRM through a combination of linear models. The proposed observer is designed based on this representation, by incorporating the sector nonlinearity approach to obtain an exact representation of the original nonlinear model.

The T-S representation of the SynRM model (2) is given as follows:

$$\begin{cases} \dot{\mathrm{x}}(\mathrm{t}) = \sum_{\mathrm{i}=1}^{\mathrm{r}} \mu_{\mathrm{i}}\left(\mathrm{x}(\mathrm{t})\right)\left(\mathrm{A}_{\mathrm{i}}\mathrm{x}(\mathrm{t}) + \mathrm{B}_{\mathrm{i}}\mathrm{u}(\mathrm{t}) + \mathrm{E}_{\mathrm{i}}\mathrm{d}(\mathrm{t})\right), \\ \mathrm{y}(\mathrm{t}) = \mathrm{C}\mathrm{x}(\mathrm{t}) + Gd(t), \end{cases} \tag{3}$$

where the known matrices are represented by $A_i \in \mathbb{R}^{n\times n}$, $B_i \in \mathbb{R}^{n\times n_u}$, $E_i \in \mathbb{R}^{n\times n_d}, C \in \mathbb{R}^{n_y\times n}$, and $G \in \mathbb{R}^{n_y\times n_d}$. Lastly, $\mu_i(x(t))$ is identified as the weighting functions that verifies the convex sum property described as follows:

$$\begin{cases} \sum_{i=1}^{r} \mu_i\left(x(t)\right) = 1, \\ 0 \le \mu_i\left(x(t)\right) \le 1, \qquad \forall i = 1,...r. \end{cases} \tag{4}$$

By identifying the premise variables $\xi_1 = i_{sq}$ and $\xi_2 = \omega$ as the nonlinear terms present in the dynamic SynRM model in (3), the weighting functions can be described as follows:

$$\begin{cases} \mu_1\left(x\left(t\right)\right) = \mathrm{W}_1\left(\xi_1\right)\mathrm{W}_1\left(\xi_2\right), \mu_2\left(x\left(t\right)\right) = \mathrm{W}_1\left(\xi_1\right)\mathrm{W}_2\left(\xi_2\right), \\ \mu_3\left(x\left(t\right)\right) = \mathrm{W}_2\left(\xi_1\right)\mathrm{W}_1\left(\xi_2\right), \mu_4\left(x\left(t\right)\right) = \mathrm{W}_2\left(\xi_1\right)\mathrm{W}_2\left(\xi_2\right). \end{cases} \tag{5}$$

And using the sector nonlinearity approach, the following functions are obtained:

$$\begin{cases} \mathrm{W}_1\left(\xi_1\right) = \frac{\xi_1 - \xi_{1\min}}{\xi_{1\max} - \xi_{1\min}}, \mathrm{W}_2\left(\xi_1\right) = \frac{\xi_{1\max} - \xi_1}{\xi_{1\max} - \xi_{1\min}}, \\ \mathrm{W}_1\left(\xi_2\right) = \frac{\xi_2 - \xi_{2\min}}{\xi_{2\max} - \xi_{2\min}}, \mathrm{W}_2\left(\xi_2\right) = \frac{\xi_{2\max} - \xi_2}{\xi_{2\max} - \xi_{2\min}}. \end{cases} \tag{6}$$

The limits of these premise variables are: $\xi_1(j) = [i_{sd_{max}} \quad i_{sd_{min}}], \xi_3(k) = [\omega_{max} \quad \omega_{min}]$. By substituting every one by its corresponding limit in a loop, it is possible to determine the sub-matrices $A_i$, $B_i$, and $E_i$ of the multimodel (4) as indicated below:

$$B_i = B, \; E_i = E, \; G = 0,$$

$$A_i = \begin{bmatrix} -\frac{R_s}{L_d} & \frac{L_q}{L_d}\xi_3(j) & 0 \\ -\frac{L_d}{L_q}\xi_3(j) & -\frac{R_s}{L_q} & 0 \\ \alpha\xi_1(k) & 0 & -\frac{f}{J_m} \end{bmatrix}, \forall i = 1...4.$$

## IV. DECOUPLED UNKNOWN INPUT OBSERVER DESIGN

The Takagi-Sugeno model of the SynRM, as outlined in the preceding section, employs unmeasurable premise variables. The design of the proposed observer will therefore tackle this particular type of system.

Let us proceed by examining the following DUIO:

$$\begin{cases} \dot{\mathrm{z}}(\mathrm{t}) = \sum_{\mathrm{i}=1}^{\mathrm{r}} \mu_{\mathrm{i}}\left(\hat{\mathrm{x}}(\mathrm{t})\right)\left(\mathrm{N}_{\mathrm{i}}\mathrm{z}(\mathrm{t}) + \mathrm{RA}_{\mathrm{i}}\hat{\mathrm{x}}(\mathrm{t}) + \mathrm{RB}_{\mathrm{i}}\mathrm{u}(\mathrm{t}) + \mathrm{F}_{\mathrm{i}}\mathrm{y}(\mathrm{t})\right), \\ \hat{\mathrm{x}}(\mathrm{t}) = \mathrm{z}(\mathrm{t}) - Hy(t). \end{cases} \tag{7}$$

The estimation error is given as follows

$$e(t) = x(t) - \hat{x}(t) = Rx(t) - z(t) + HGd(t), \tag{8}$$

where

$$R = I + HC. \tag{9}$$

Therefore, the estimation error dynamics is given by

$$\dot{e}(t) = \sum_{i=1}^{r} \mu_i\left(\hat{x}(t)\right)\mathcal{H}(\mathrm{t}) + HG\dot{d}(t) + R\left(\Phi(x) - \Phi(\hat{x})\right), \tag{10}$$

where:

$$\mathcal{H}(\mathrm{t}) = \left(-N_iR - F_iC\right)x + \left(RE_i - \left(F_i + N_iH\right)G\right)d + N_ie, \tag{11}$$

$$\Phi(x) = \sum_{i=1}^{r} \mu_i\left(x(t)\right)\left[A_ix(t) + B_iu(t) + E_id(t)\right]. \tag{12}$$

By using the change of variable $K_i = N_iH + F_i$ and verifying the conditions (13) to (15):

$$HG = 0, \tag{13}$$

$$N_i = -K_iC, \tag{14}$$

$$RE_i = K_iG. \tag{15}$$

The error dynamics is then given by

$$\dot{e}(t) = \sum_{i=1}^{r} \mu_i\left(\hat{x}(t)\right)N_ie(t) + R\left(\Phi(x) - \Phi(\hat{x})\right). \tag{16}$$

*Lemma 1*: [25] Let $\Phi(x)$: $R^n => R^n$ be a vector function with $\Phi_i(x)$: $\mathbb{R}^n => \mathbb{R}$ its $i^{th}$ component. By assuming that $\Phi(x)$ is differentiable, then there are constant vectors $z1$, …, $zn \in (a, b), zi \neq a, zi \neq b$ for $i = 1, \ldots, n$ such that

$$\Phi(a) - \Phi(b) = \sum_{i=1}^{n}\sum_{j=1}^{n} e_n(i)e_n(j)^T \frac{\partial\Phi_i\left(z_j\right)}{\partial x_j}(a - b), \tag{17}$$

where $En$ is the canonical basis of the vectorial space $\mathbb{R}^n$ for all $n \geq 1$

$$En = \left\{ e_n(i) \middle| e_n(i) = \left( 0,...,0,\underset{\text{i}}{1},0,...,0 \right)^T, i = 1,...,n \right\}. \quad (18)$$

Applying the T-S representation, the following form is obtained

$$\Phi(a) - \Phi(b) = \sum_{j=1}^{q} h_j\left(z(t)\right) \mathcal{A}_j (a-b). \quad (19)$$

$\mathcal{A}_j$ indicates the sub-model corresponding to the nonlinear component $\sum_{i=1}^{n}\sum_{j=1}^{n} e_n(i) e_n(j)^T \frac{\partial \Phi_i(z_j)}{\partial x_j}$ and $h_i(z(t))$ represents its weighting functions, whereas $q$ signifies the total number of sub-models.

Using the differential mean value theorem described in Lemma 1, the term $(\Phi(x) - \Phi(\hat{x}))$ is given by (19); therefore, the error dynamics becomes

$$\dot{e}(t) = \sum_{i=1}^{r}\sum_{j=1}^{q} \mu_i\left(\hat{x}(t)\right) h_i\left(z(t)\right)\left(N_i + R\mathcal{A}_j\right) e(t). \quad (20)$$

Based on the work presented in [26], the following theorem provides sufficient conditions to guarantee the asymptotic convergence of the error dynamics (20).

*Theorem 1*: The estimation error converges asymptotically toward zero with the decay rate $\alpha$ if there exist matrices $P = P^T \in \mathbb{R}^{n_x \times n_x} > 0, M_i \in \mathbb{R}^{n_x \times n_y}$, and $S \in \mathbb{R}^{n_x \times n_y}$ such that the following conditions holds $\forall\ i = 1, \ldots, r$ and $j = 1, \ldots, q$:

$$\left(P\mathcal{A}_j + SC\mathcal{A}_j - M_i C\right)^T + \left(P\mathcal{A}_j + SC\mathcal{A}_j - M_i C\right) < -2\alpha P, \quad (21)$$

$$SG = 0, \quad (22)$$

$$(P + SC) E_i = M_i G. \quad (23)$$

The observer matrices are given by:

$$H = P^{-1} S, \quad (24)$$

$$K_i = P^{-1} M_i, \quad (25)$$

$$N_i = -K_i C, \quad (26)$$

$$F_i = K_i - N_i H. \quad (27)$$

*Proof*: Let us define the quadratic Lyapunov function as

$$V(t) = e(t)^T P e(t). \quad (28)$$

The time derivative of $V(t)$ is

$$\dot{V}(t) = \dot{e}(t)^T P e(t) + e(t)^T P \dot{e}(t). \quad (29)$$

By substituting (20) in (29), (30) is obtained

$$\dot{V}(t) = \sum_{i=1}^{r}\sum_{j=1}^{q} \mu_i\left(\xi(t)\right) h_j\left(z(t)\right) \times$$
$$\times \left[ \left(P\mathcal{A}_j + PHC\mathcal{A}_j - PK_i C\right)^T + \left(P\mathcal{A}_j + PHC\mathcal{A}_j - PK_i C\right) \right]. \quad (30)$$

By using the following change of variables:

$$S = PH, \quad (31)$$

$$M_i = PK_i, \quad (32)$$

coupled with the decay rate expressed as

$$\dot{V}(t) < -2\alpha P, \quad (33)$$

the inequalities outlined in (21) of Theorem 1 are obtained. Integrating (31) with (13), (22) is obtained. Furthermore, combining (31) and (32) with (15) results in (23).

## V. UNKNOWN INPUT ESTIMATION

After completing the state estimation and effectively isolating the impact of the UI on the estimation error, the UI can be deduced using the estimated state vector.

In the context of system (3), the UI is present alongside its associated influence matrix

$$W(t) = \begin{bmatrix} \sum_{i=1}^{r} \mu_i\left(\hat{x}(t)\right) E_i \\ G \end{bmatrix}. \quad (34)$$

Therefore, the UI can be deduced using the following equation

$$\hat{d}(t) = W^{-}(t) \begin{bmatrix} \dot{\hat{x}}(t) - \sum_{i=1}^{r} \mu_i\left(\hat{x}(t)\right)\left(A_i \hat{x}(t) + B_i u(t)\right) \\ y\left(t - C\hat{x}(t)\right) \end{bmatrix}, \quad (35)$$

where $W^{-}(t)$ is left pseudo-inverse of $W(t)$ that exists if the following condition is verified at every instant $t$

$$rank\left(W(t)\right) = n_d, \quad (36)$$

where $n_d$ is the dimension of the UI vector, and $W^{-}(t)$ is given in the following equation

$$W^{-}(t) = \left(W^T(t) W(t)\right)^{-1} W^T(t). \quad (37)$$

## VI. OBSERVER DESIGN FOR SYNCHRONOUS RELUCTANCE MOTOR

This section outlines the process of determining the gain of the DUIO applied to the SynRM. To validate Theorem 1, it is necessary to first identify the $\mathcal{A}_i$ terms.

Since that $\forall i = 1 \ldots 4$, the matrices $B_i$ are identical, as well as for $E_i$, then the value of $\Phi(x)$ in (12) can be reduced to

$$\Phi(x) = \sum_{i=1}^{r} \mu_i\left(x(t)\right)\left[A_i x(t)\right] = A(x) x. \quad (38)$$

According to Lemma 1, the MVT is applied as follows

$$\frac{\partial A(x) x}{\partial x} = \begin{bmatrix} -\frac{R_s}{L_d} & \frac{L_q}{L_d}\omega & \frac{L_q}{L_d} i_{sq} \\ -\frac{L_d}{L_q}\omega & -\frac{R_s}{L_q} & -\frac{L_d}{L_q} i_{sd} \\ \alpha i_{sq} & \alpha i_{sd} & -\frac{f}{Jm} \end{bmatrix},$$

By defining the limits of the premise variables as: $\xi_1(j) = [i_{sd_{max}} \quad i_{sd_{min}}], \xi_2(k) = [i_{sq_{max}} \quad i_{sq_{min}}]$, and $\xi_3(d) = [\omega_{max} \quad \omega_{min}]$, and by employing the T-S representation along with the sector nonlinearity approach on $\frac{\partial A(x)x}{\partial x}$, the terms $\mathcal{A}_i$ can be obtained by substituting every premise variable by its corresponding limit in a loop as follows

$$\mathcal{A}_i = \begin{bmatrix} -\frac{R_s}{L_d} & \frac{L_q}{L_d}\xi_3(d) & \frac{L_q}{L_d}\xi_2(k) \\ -\frac{L_d}{L_q}\xi_3(d) & -\frac{R_s}{L_q} & -\frac{L_d}{L_q}\xi_1(j) \\ \alpha\xi_2(k) & \alpha\xi_1(j) & -\frac{f}{Jm} \end{bmatrix}.$$

Taking into account the output as $y(t) = \omega(t)$, and using a decay rate of $\alpha = 6.5$, Theorem 1 is used to deduce the observer gain for the DUIO of the SynRM:

$$N_i = \begin{bmatrix} 0 & 0 & 0.0020 \\ 0 & 0 & 0.0592 \\ 0 & 0 & -8.4650 \end{bmatrix}, \; F_i = \begin{bmatrix} 9.5410\times10^{-18} \\ 2.9143\times10^{-16} \\ -4.0856\times10^{-14} \end{bmatrix}, \; \forall i = 1...8,$$

$$H = \begin{bmatrix} 0 \\ 0 \\ 0 \\ -1 \end{bmatrix}, \; R = \begin{bmatrix} 1 & 0 & 0 \\ 0 & 1 & 0 \\ 0 & 0 & 0 \end{bmatrix},$$

$$P = \begin{bmatrix} 0.2304 & 0 & 0 \\ 0 & 0.0164 & 0 \\ 0 & 0 & 6.8698 \end{bmatrix} \times 10^3.$$

The motor parameters are given by the following: Rated power $P_r = 2.2$ [kW], Rated voltage $V_r = 220/380$ [V], Rated speed $\Omega_r = 1500$ [rpm], Stator resistance $R_s = 1.71$ [Ω], Inductance of direct axis $L_d = 0.15$ [H], Inductance of quadratic axis $L_q = 0.04$ [H], Moment of inertia $J = 0.0137$ [kg × m$^2$], Number of pair of poles $p = 2$, and Viscous friction $f = 0.00036$ [Nm/rad/s].

## VII. HARDWARE-IN-THE-LOOP VALIDATION

This section presents an experimental test conducted to validate the effectiveness of the proposed DUIO. The evaluation is split into two subsections. The first subsection focusses on assessing the effectiveness of the state and UI estimation of the proposed observer. The second subsection offers a comparative analysis in the context of UI estimation of DUIO against PIO, previously introduced in [17], and PMIO, proposed in [18]. The UI observer is integrated within the indirect field-orientated control strategy that manages the operation of the SynRM in these experiments. The speed regulator used is of the "IP" type with $K_{P\Omega} = 5.7070$ and $K_{I\Omega} = 156.9792$, and the current regulation is of the "PI" type with $K_{Pi} = 86.8056$ and $K_{Ii} = 989.5833$.

Figure 1 shows the overall HIL architecture employed in the experiment.

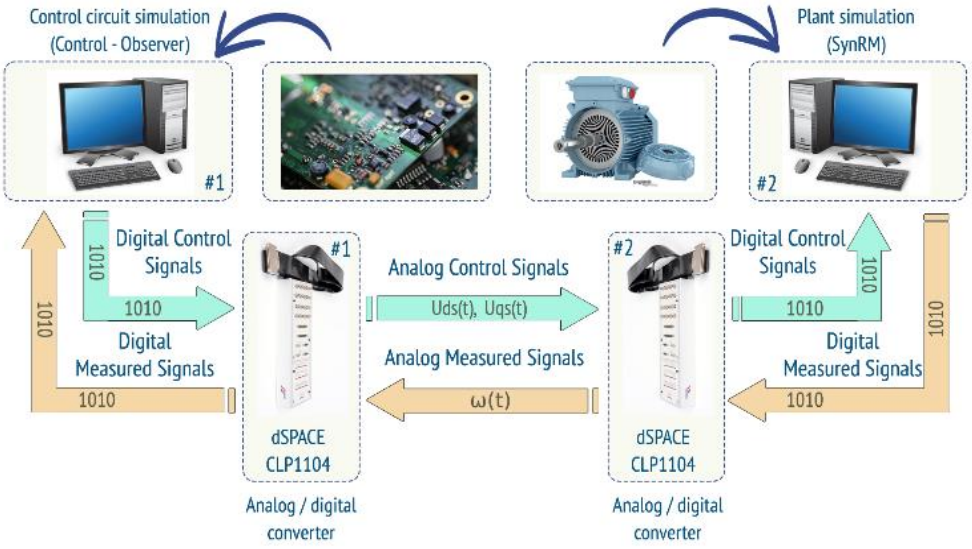


Fig. 1. Hardware-in-the-loop architecture.

This configuration used two Dspace 1104 cards, operating with a sampling time of $T_s = 0.0001$ (s). The initial card was tasked with emulation of both the observer and the control circuit. Concurrently, the secondary card was exclusively dedicated to the emulation of SynRM. Figure 2 shows the experimental setup developed within the MSE Laboratory.

### A. Evaluation of Decoupled Unknown Input Observer Performance

The experiment proceeded by using the speed profile depicted in Fig. 3, in conjunction with a flux reference set to 0.8 (Wb). To substantiate the stability of the error dynamics, the system's initial conditions were configured as $x_0(t) = [-1 \quad 2 \quad 50]$. Figures 3 through 6 present the outcome of the state estimate. Furthermore, Figure 7 illustrates the UI profile and its estimation, while its estimation error is clearly represented by Fig. 8.

The results shown in Figs. 3 through 8, along with those of Table I, demonstrate the successful estimation by the observer of the SynRM states despite disturbances in information transmission between the two platforms and differences in initial conditions between the system and the observer.

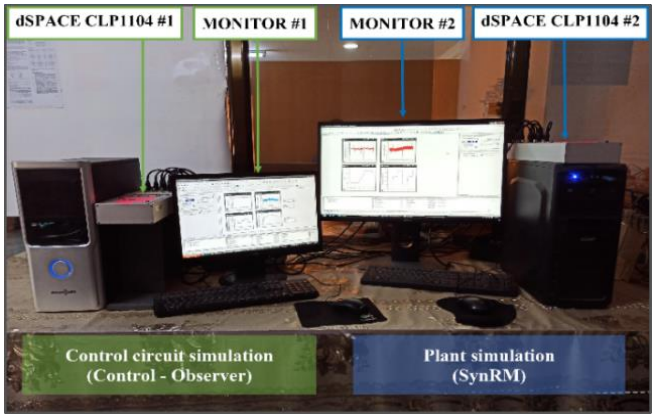


Fig. 2. Hardware in-the-loop test bench.

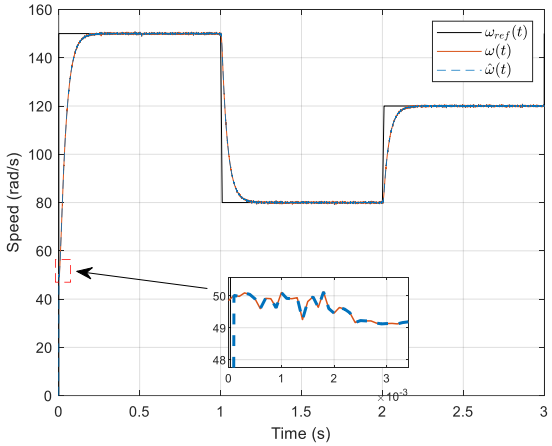


Fig. 3. Rotor angular speed curve.

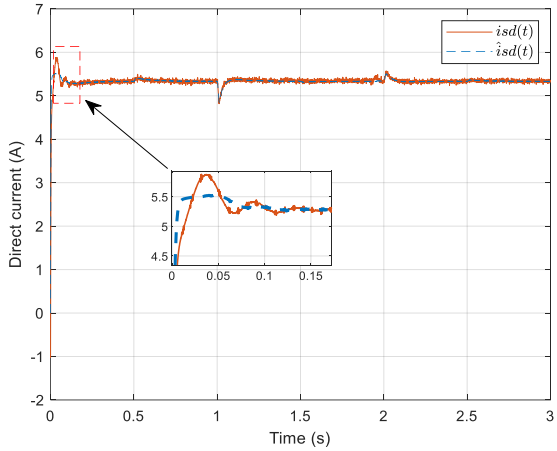


Fig. 4. Direct axis stator current.

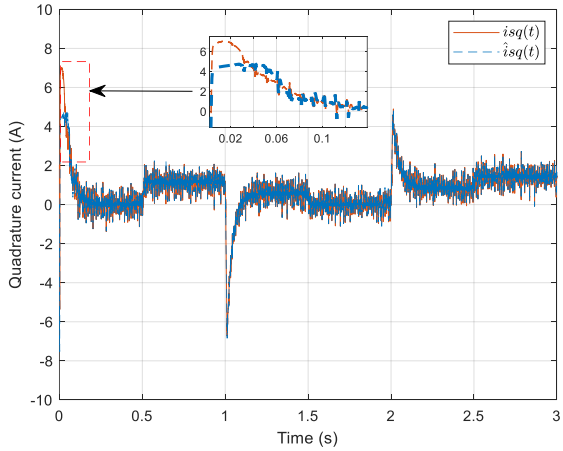


Fig. 5. Quadrature axis stator current.

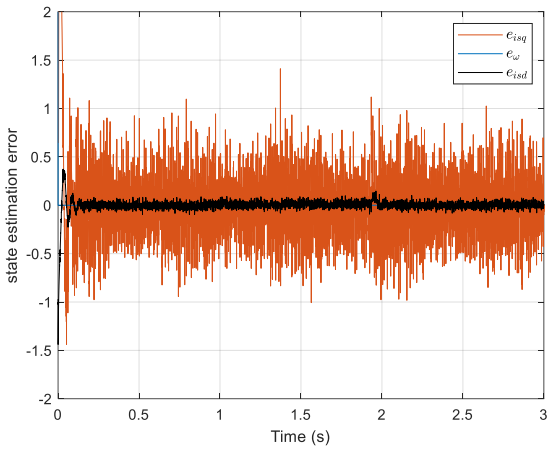


Fig. 6. State estimation error.

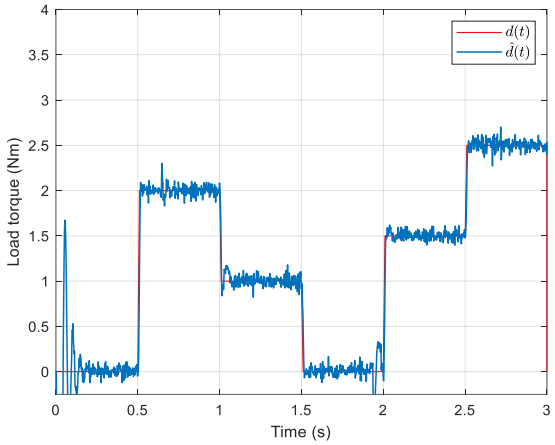


Fig. 7. Unknown input estimation.

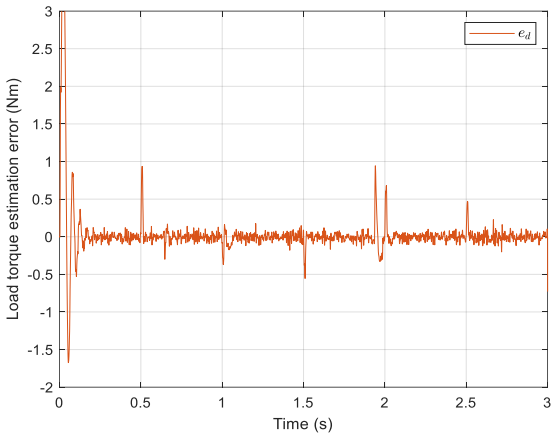


Fig. 8. Unknown input estimation error.

TABLE I. STATE ESTIMATION PERFORMANCE.

| Observer performance | Integral Square Error | Integral Absolute Error | Mean squared error |
|---|---|---|---|
| $e_{i_{sd}}(A)$ | 0.0074 | 0.0588 | 0.0019 |
| $e_{i_{sq}}(A)$ | 0.2339 | 0.4289 | 0.0585 |
| $e_d$(Nm) | 0.4360 | 0.3779 | 0.1089 |

This effective state estimation, even under varying initial conditions, highlights the robustness and adaptability of our observer under challenging real-time application conditions. A further significant observation, illustrated by Fig. 7, is the observer's ability to adeptly handle the varying nature of the UI. Even with these variations, the observer's estimation of this UI was tracked perfectly, with only minor errors that

remained within acceptable limits. This strong performance in the presence of UI changes significantly emphasises the overall reliability of the proposed observer.

### B. *Comparative Results*

In this section, a comparative assessment is performed to evaluate the performance of the proposed DUIO observer against PIO and PMIO observers. The examination is centred on the ability of these observers to estimate UI under various conditions: slow, fast, and random UI variations. The ensuing results will highlight their adaptability and effectiveness, thereby offering a more comprehensive understanding of their potential utility in real-world applications.

The observer gains obtained from PIO are given by:

$$L_p = \begin{bmatrix} 8.2961\times10^{-11} \\ -3.0162\times10^{-12} \\ 1.2254\times10^{+4} \end{bmatrix},\ L_I = \begin{bmatrix} -1.4678\times10^{+3} \end{bmatrix},$$

and those for PMIO of order q = 3 (P3IO), are given by:

$$L_p = \begin{bmatrix} 8.5621\times10^{-12} \\ -5.8990\times10^{-12} \\ 1.3533\times10^{+4} \end{bmatrix},\ L_I = \begin{bmatrix} -4.7362\times10^{3} \\ -6.1513\times10^{4} \\ -2.6645\times10^{5} \end{bmatrix}.$$

### C. *Case 1 (Slow Unknown Input Variation)*

A thorough comparative analysis involving DUIO, PMIO, and PIO was conducted under slow variations conditions of the UI. Figure 9 represents the actual UI and its corresponding estimations. Table II shows the various performance criteria for the estimation error. In these circumstances, it was found that the proposed observer had the best performance and lowest error criterion among the three observers.

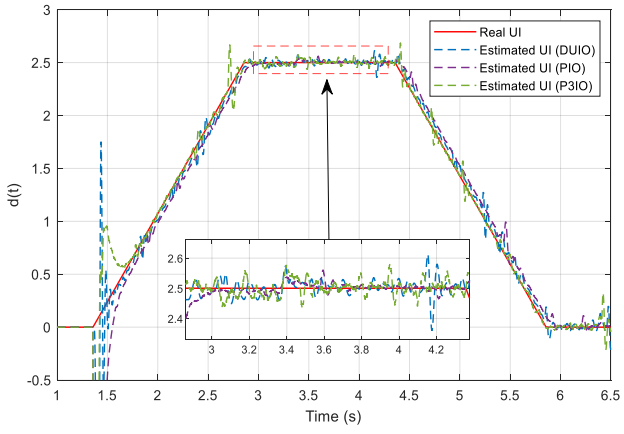


Fig. 9. Unknown input estimation (case 1).

TABLE II. UNKNOWN INPUT ESTIMATION PERFORMANCE (CASE 1).

| Observer | Integral Square Error | Integral Absolute Error | Mean squared error |
|---|---|---|---|
| PIO | 1.6015 | 0.7519 | 0.2669 |
| P3IO | 1.5907 | 0.5422 | 0.2651 |
| **DUIO** | **0.4841** | **0.4198** | **0.0807** |

Although primarily designed to estimate UIs with null derivatives, the PIO remarkably managed to effectively accommodate inputs with slow variations, essentially considering their derivatives as null. PMIO markedly demonstrated a good fit with this type of UI. Given its original design to handle unknown variable inputs, it is entirely expected that the PMIO performs well with simpler, slower variations. Moreover, the DUIO, although it did not consider the form of the UI during its design process, demonstrated its robustness and adaptability by providing a commendable estimation, thus highlighting the strength of its design.

### D. *Case 2 (Fast Unknown Input Variation)*

This experiment, precisely configured for situations where the variation in the UI is fast, gives insight into the distinctive performances of PIO, PMIO, and DUIO. Figure 10 offers a detailed illustration of both the actual UI and its respective estimates, while Table III outlines a range of performance criteria related to the estimation error of the UI. The PIO, as shown, struggled with fast changes in the UI, thus exposing its limitations in these situations. In contrast, the PMIO, whose design is fundamentally conceived to handle such variations, demonstrated significant adaptability and performance. However, there was a noticeable, though slight, drop in PMIO performance during the phase when the UI moved from a horizontal to a diagonal form. The increased derivative at this moment exceeds what the observer was originally designed for. Even so, the PMIO recovered quickly, managing to reduce the estimation error promptly. Under these conditions, the performance disparity between these observers became considerably more pronounced, a contrast further elaborated in Table III. Meanwhile, the proposed DUIO consistently performed at a high level, much as in the first experiment. The resulting estimates aligned closely with the original UI, despite its rapid variation, illustrating once again the effectiveness of the DUIO in providing accurate estimates in various scenarios.

TABLE III. UNKNOWN INPUT ESTIMATION PERFORMANCE (CASE 2).

| Observer | Integral Square Error | Integral Absolute Error | Mean squared error |
|---|---|---|---|
| PIO | 0.4610 | 0.8667 | 0.1537 |
| P3IO | 0.0535 | 0.2930 | 0.0178 |
| **DUIO** | **0.0120** | **0.1452** | **0.0040** |

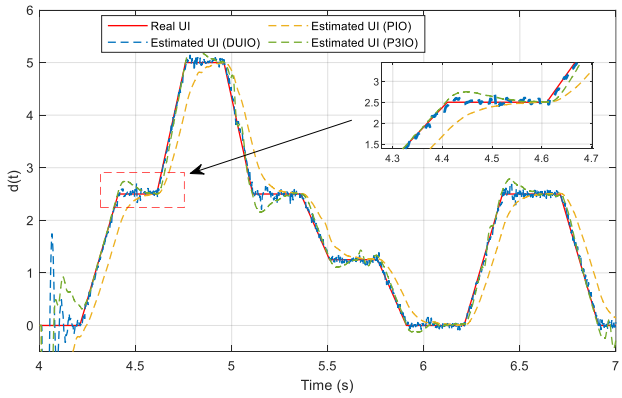


Fig. 10. Unknown input estimation (case 2).

### E. Case 3 (Random Unknown Input Variation)

In the third examination performance test, visualised in Fig. 11 and quantified in Table IV, the UI displayed an unpredictable and random pattern, thereby posing a rigorous challenge for the three observers. Both PIO and PMIO experienced diminished performance, as the unexpected variability in the UI outpaced what these observers were initially designed to manage. However, even within this complex environment, PMIO maintained a level of performance that surpassed PIO, showcasing its resilience amidst unpredictable variations. Concurrently, the proposed DUIO preserved its consistent high performance and remarkable accuracy, deftly managing the random form of the UI. This experiment reaffirmed the effectiveness of the robust DUIO design, demonstrating its ability to flexibly accommodate various forms and fluctuations of UIs. In comparison, the constrained performances of PIO and PMIO were highlighted, emphasising their limitations when faced with scenarios that their specific designs did not account for.

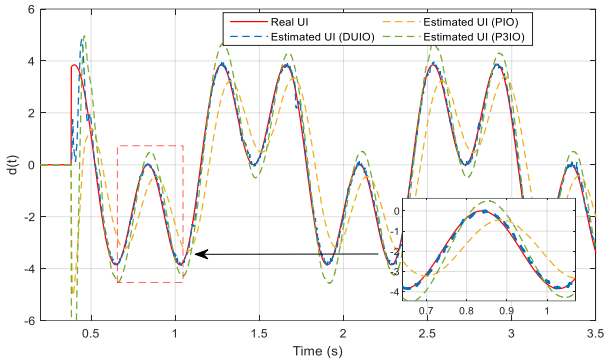


Fig. 11. Unknown input estimation (case 3).

TABLE IV. UNKNOWN INPUT ESTIMATION PERFORMANCE (CASE 3).

| Observer | Integral Square Error | Integral Absolute Error | Mean squared error |
|---|---|---|---|
| PIO | 6.0136 | 2.3199 | 3.5114 |
| P3IO | 4.1586 | 1.3628 | 2.4282 |
| **DUIO** | **0.0889** | **0.2012** | **0.0519** |

## VIII. CONCLUSIONS

This work highlights a notable advancement in the estimation of UIs applicable to synchronous reluctance motors, validated through hardware-in-the-loop experimentation. The proposed DUIO showed a significant improvement over the previously implemented PIO and PMIO in terms of precision under different conditions. The capacity of the UI estimation was rigorously tested under three distinct scenarios: slow, rapid, and random variations. Across all these conditions, the DUIO had best performance and lowest error criterion among the other observers, consistently demonstrated its superiority, outperforming the other observers and proving its robust design, which proved adaptable to various forms and fluctuations of UIs. This work not only reaffirms the effectiveness of DUIO, but also highlights its potential for broader application in similar scenarios. Building on this success, future work can delve into the design of feedforward and fault-tolerant control strategies, aiming to further improve the overall performance of the control system.

## CONFLICTS OF INTEREST

The authors declare that they have no conflicts of interest.

## REFERENCES

[1] H. Heidari *et al.*, "A review of synchronous reluctance motor-drive advancements", *Sustainability*, vol. 13, no. 2, p. 729, 2021. DOI: 10.3390/su13020729.

[2] G. V. Kumar, C.-H. Chuang, M.-Z. Lu, and C.-M. Liaw, "Development of an electric vehicle synchronous reluctance motor drive", *IEEE Transactions on Vehicular Technology*, vol. 69, no. 5, pp. 5012–5024, 2020. DOI: 10.1109/TVT.2020.2983546.

[3] A. Credo, G. Fabri, M. Villani, and M. Popescu, "Adopting the topology optimization in the design of high-speed synchronous reluctance motors for electric vehicles", *IEEE Transactions on Industry Applications*, vol. 56, no. 5, pp. 5429–5438, 2020. DOI: 10.1109/TIA.2020.3007366.

[4] V. Kazakbaev, V. Prakht, V. Dmitrievskii, M. N. Ibrahim, S. Oshurbekov, and S. Sarapulov, "Efficiency analysis of low electric power drives employing induction and synchronous reluctance motors in pump applications", *Energies*, vol. 12, no. 6, p. 1144, 2019. DOI: 10.3390/en12061144.

[5] M. N. Ibrahim, H. Rezk, M. Al-Dhaifallah, and P. Sergeant, "Solar array fed synchronous reluctance motor driven water pump: An improved performance under partial shading conditions", *IEEE Access*, vol. 7, pp. 77100–77115, 2019. DOI: 10.1109/ACCESS.2019.2922358.

[6] N. G. Ozcelik, U. E. Dogru, M. Imeryuz, and L. T. Ergene, "Synchronous reluctance motor vs. induction motor at low-power industrial applications: Design and comparison", *Energies*, vol. 12, no. 11, p. 2190, 2019. DOI: 10.3390/en12112190.

[7] H. H. Alhelou, M. E. H. Golshan, and J. Askari-Marnani, "Robust sensor fault detection and isolation scheme for interconnected smart power systems in presence of RER and EVs using unknown input observer", *International Journal of Electrical Power & Energy Systems*, vol. 99, pp. 682–694, 2018. DOI: 10.1016/j.ijepes.2018.02.013.

[8] F. Pourdadashi Komachali and M. Shafiee, "Sensor fault diagnosis in fractional-order singular systems using unknown input observer", *International Journal of Systems Science*, vol. 51, no. 1, pp. 116–132, 2020. DOI: 10.1080/00207721.2019.1701135.

[9] Y. Wu, D. Du, Z. Mao, and Y. Yang, "A novel unknown input observer-based fault detection with application to a two-stage chemical reactor", *International Journal of Adaptive Control and Signal Processing*, vol. 35, no. 9, pp. 1789–1804, 2021. DOI: 10.1002/acs.3292.

[10] R. E. Kalman, "A new approach to linear filtering and prediction problems", *J. Basic Eng.*, vol. 82, no. 1, pp. 35–45, 1960. DOI: 10.1115/1.3662552.

[11] D. G. Luenberger, "An introduction to observers", *IEEE Transactions on Automatic Control*, vol. 16, no. 6, pp. 596–602, 1971. DOI: 10.1109/TAC.1971.1099826.

[12] K. Tanaka and H. O. Wang, *Fuzzy Control Systems Design and Analysis: A Linear Matrix Inequality Approach*. John Wiley & Sons, Inc., 2001. DOI: 10.1002/0471224596.

[13] S.-H. Tsai and Y.-W. Chen, "A novel identification method for Takagi-Sugeno fuzzy model", *Fuzzy Sets and Systems*, vol. 338, pp. 117–135, 2018. DOI: 10.1016/j.fss.2017.10.012.

[14] W. Qi, C. Lv, G. Zong, and C. K. Ahn, "Sliding mode control for fuzzy networked semi-Markov switching models under cyber attacks", *IEEE Transactions on Circuits and Systems II: Express Briefs*, vol. 69, no. 12, pp. 5034–5038, 2022. DOI: 10.1109/TCSII.2021.3137196.

[15] F.-R. López-Estrada, D. Rotondo, and G. Valencia-Palomo, "A review of convex approaches for control, observation and safety of linear parameter varying and Takagi-Sugeno systems", *Processes*, vol. 7, no. 11, p. 814, 2019. DOI: 10.3390/pr7110814.

[16] S. Abdelmalek, A. T. Azar, and D. Dib, "A novel actuator fault-tolerant control strategy of DFIG-based wind turbines using Takagi-Sugeno multiple models", *International Journal of Control, Automation and Systems*, vol. 16, no. 3, pp. 1415–1424, 2018. DOI: 10.1007/s12555-017-0320-y.

[17] A. Boukhlouf, M. Y. Hammoudi, R. Saadi, and M. E. H. Benbouzid, "Hardware-in-the-loop implementation of an unknown input observer for synchronous reluctance motor", *ISA Transactions*, vol. 133, pp. 485–494, 2023. DOI: 10.1016/j.isatra.2022.07.008.

[18] W. Hamdi *et al.*, "Enhanced state and unknown input estimation for synchronous reluctance motor using Takagi-Sugeno fuzzy proportional multi-integral observer", *IEEE Access*, vol. 12, pp.

42908–42920, 2024. DOI: 10.1109/ACCESS.2024.3378583.
[19] A. S. Hadi, M. S. Shaker, and Q. A. Jawad, "Estimation/decoupling approach for robust Takagi-Sugeno UIO-based fault reconstruction in nonlinear systems affected by a simultaneous time varying actuator and sensor faults", *International Journal of Systems Science*, vol. 50, no. 13, pp. 2473–2485, 2019. DOI: 10.1080/00207721.2019.1671528.
[20] V.-P. Vu, W.-J. Wang, J. M. Zurada, H.-C. Chen, and C.-H. Chiu, "Unknown input method based observer synthesis for a discrete time uncertain T-S fuzzy system", *IEEE Transactions on Fuzzy Systems*, vol. 26, no. 2, pp. 761–770, 2018.
[21] A. A. Memon and K. Kauhaniemi, "Real-time hardware-in-the-loop testing of IEC 61850 GOOSE-based logically selective adaptive protection of AC microgrid", *IEEE Access*, vol. 9, pp. 154612–154639, 2021. DOI: 10.1109/ACCESS.2021.3128370.
[22] J. A. G. Archetti *et al.*, "Real time validation of a control system for microgrids with distributed generation and storage resources", *Electric Power Systems Research*, vol. 223, art. 109683, 2023. DOI: 10.1016/j.epsr.2023.109683.
[23] L. Zhang, H. Zhang, H. Obeid, and S. Laghrouche, "Time-varying state observer based twisting control of linear induction motor considering dynamic end effects with unknown load torque", *ISA Transactions*, vol. 93, pp. 290–301, 2019. DOI: 10.1016/j.isatra.2019.03.008.
[24] T. Sharaf-Eldin, M. W. Dunnigan, J. E. Fletcher, and B. W. Williams, "Nonlinear robust control of a vector-controlled synchronous reluctance machine", *IEEE Transactions on Power Electronics*, vol. 14, no. 6, pp. 1111–1121, 1999. DOI: 10.1109/63.803405.
[25] K. Mimoune, M. Y. Hammoudi, R. Saadi, M. Benbouzid, and A. Boukhlouf, "Real-time implementation of non linear observer based state feedback controller for induction motor using mean value theorem", *Journal of Electrical Engineering & Technology*, vol. 18, no. 1, pp. 615–628, 2023. DOI: 10.1007/s42835-022-01274-1.
[26] D. Ichalal and T.-M. Guerra, "Decoupling unknown input observer for nonlinear quasi-LPV systems", in *Proc. of 2019 IEEE 58th Conference on Decision and Control (CDC)*, 2019, pp. 3799–3804. DOI: 10.1109/CDC40024.2019.9029339.